

Journal of  
**Micro/Nanolithography,  
MEMS, and MOEMS**

SPIEDigitalLibrary.org/jm3

# **Microlight-emitting diode with integrated Fresnel zone plate for contact lens embedded display**

Ramin Mirjalili  
Babak A. Parviz



# Microlight-emitting diode with integrated Fresnel zone plate for contact lens embedded display

Ramin Mirjalili

Babak A. Parviz

University of Washington

Department of Electrical Engineering

185 Stevens Way, Paul Allen Center

Campus Box 352500

Seattle, Washington 98195-2500

E-mail: [ramin@u.washington.edu](mailto:ramin@u.washington.edu)

**Abstract.** We report the fabrication and testing of 30- $\mu\text{m}$  radii circular InGaN blue light-emitting diode (LEDs) grown on sapphire wafers, with cointegrated Fresnel zone plates (FZP) with outermost ring radii of 99.6  $\mu\text{m}$  on the backside of the sapphire substrates to provide a collimated output. After being embedded on a contact lens platform such LEDs with integrated lenses can aid in producing in-focus images on the human retina. We measured an image width of 50  $\mu\text{m}$  created by a FZP  $f/3$  subsidiary focal point at 230  $\mu\text{m}$  from the surface. We also demonstrate the construction and wireless operation of a contact lens with predetermined embedded text. © 2012 Society of Photo-Optical Instrumentation Engineers (SPIE). [DOI: [10.1117/1.JMM.11.3.033010](https://doi.org/10.1117/1.JMM.11.3.033010)]

Subject terms: contact lens; Fresnel zone plate; microlight-emitting diode; wearable display.

Paper 12013 received Feb. 13, 2012; revised manuscript received Jul. 21, 2012; accepted for publication Jul. 31, 2012; published online Sep. 21, 2012.

## 1 Introduction

Wearable devices, such as various health monitoring and entertainment systems, could soon alter our interactions with the surrounding environment and the computing cloud. For example personal see-through displays could in principle overlay computer-generated visual information on the real world, providing immediate, hands-free access to information.<sup>1</sup> Such displays may be realized in the form of devices resembling eyewear for vision correction or even contact lenses that can be remotely powered and controlled to show information (Fig. 1). In a sample embodiment, the contact lens may integrate an array of microlight-emitting diode (LEDs) for producing images. We have previously reported the functionality of wirelessly controlled single pixel display on a contact lens platform.<sup>2,3</sup> Such a single pixel system may be deployed for communicating immediate events to the user however it is of limited use for conveying more information. Our custom designed wireless system could deliver 12  $\mu\text{W}$  of power to the display, harvested from a 0 dBm (1 mW) radio frequency (RF) broadcast source and used 3% modulation for power management.<sup>2</sup> In our prior demonstration, the nominal visibility point for the InGaN LED (60  $\mu\text{A}$  of current at 2.6 V for a 260- $\mu\text{m}$  wide pixel),<sup>3</sup> translated to approximately 2.94  $\text{nW}/\mu\text{m}^2$ , this in turn means the system as deployed could support up to nearly 50 pixels made of 30- $\mu\text{m}$  wide LEDs should the proper pixel design and optics becomes available.

A major challenge of constructing a display wearable in the form of a contact lens with multiple pixels is producing in-focus images from components that are placed directly on the cornea. As the nearest focus point of the human eye (closest point of accommodation) ranges from 7 to 40 cm for teenagers to middle aged adults,<sup>4</sup> the output light of micro-LED pixels on the contact lens will not be in-focus on the retina. Therefore, optical components are needed in

between the micro-LED pixels and the retina to bring the image into focus. One approach is to use a micro lens for each pixel or group of pixels to aid in focusing the light emergent from them on the retina.

The simplest way to collimate the output light of a source is to position the source at the focal point of a lens. Integration of micro lenses on micro-LEDs to enhance the extraction of LED optical output has been previously reported.<sup>5–7</sup> Micro lenses reported were based on either fabrication by reflow of transparent photoresist patterns acting as the lens,<sup>5–7</sup> or followed by an extra etch step to pattern the substrate with the lens shape.<sup>8,9</sup> Micro lenses fabricated in this manner do not give sufficient variation of focal distance nor can their focal point and other optical properties be easily controlled. Additionally these approaches would not work when the lens is embedded in a material with a similar (or very close) index of refraction, which in the case for the contact lens is the tear film next to the cornea. To minimize this effect and have a better control on focal distance, which is critical to collimate the output light, we use diffraction-based Fresnel zone plate lenses (FZP).

We report how LEDs with integrated FZP acting as a lens can be designed, fabricated, and tested. These devices pave the way for constructing a contact lens display that is capable of producing in-focus images. The following sections outline the design parameters for the FZP, the fabrication process for building the devices, and the characterization results. Finally, we briefly discuss the construction of a wirelessly powered and controlled contact lens incorporating a predetermined text.

## 2 Design and Simulation

### 2.1 Fresnel Zone Plates

FZPs are used as x-ray optical components<sup>10</sup> or lithographic patterning elements.<sup>11</sup> Their behavior is based on utilizing diffraction from circular gratings to focus the incident light to a point. If we block or give a  $\pi$  phase change at boundary radii  $R_n$ , given by Eq. (1),<sup>12</sup> the zone plate

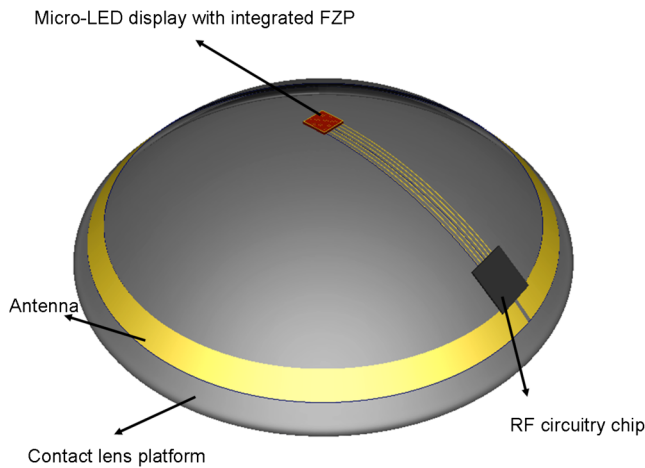


**Fig. 1** Conceptual drawing of a contact lens with embedded micro-LED display, antenna and RF circuit for powering and communication.

will act as a lens with first order focal point of  $f$  and subsidiary focal points at odd fractions of  $f$ <sup>12</sup>:

$$R_n^2 = (n\lambda f + n^2\lambda^2/4). \quad (1)$$

The less complicated way to fabricate a FZP is to eliminate the destructive interference from the incident wavefront with an opaque material (amplitude-type zone plates). Here, 50% of the incident light is blocked by the FZP surface initially and only 10% of incident light is focused on the 1st order focal point. If the opaque rings are replaced with a transparent material causing a  $\pi$  phase shift, thus making the interference constructive at the focal point (phase-type zone plates) more efficiency may be gained at the expense of additional complexity of the fabrication process. As there is no absorption in the optical path in this case, the amplitude at the focal point could be doubled, so the diffraction efficiency at 1st order focal point could be increased to 40%.<sup>12</sup> As an initial proof of concept, here we chose to fabricate amplitude-type zone plates to simplify the fabrication process.

## 2.2 Design

To collimate the LED light output, the source should be positioned at the main focal point of the FZP. In our design, FZPs were integrated on the opposite side of sapphire wafers supporting the LED epitaxial layers on the surface; hence, the wafer thickness determined the required focal distance of the

lens. Our LED peak wavelength is 475 nm<sup>3</sup>, and the wafer thickness (i.e., FZP focal distance) was approximately 275  $\mu\text{m}$  after lapping and polishing. Considering the wavelength and focal point in zone plate behavior, given by Eq. (1), we calculated the respective zone radii up to 99.6  $\mu\text{m}$ .

## 2.3 Simulation

We conducted two simulation approaches in ZEMAX-EE. First, we simulated the FZP and its focusing behavior, and second, we simulated the LED structure with integrated FZP. In the first approach, in order to model diffractive effects, we used physical optics propagation (POP) analysis of sequential mode ZEMAX. We implemented our opaque zones of FZP as concentric obscurations [Fig. 2(a)], and used a coherent Gaussian beam with 60- $\mu\text{m}$  waist and 475-nm wavelength as an illumination source. The zone plate created a high intensity point at focal distance of 275  $\mu\text{m}$  as expected [Fig. 2(b)].

To model the InGaN LED structure, we used the non-sequential mode of ZEMAX. Nonsequential mode is not capable of modeling amplitude FZP, while it can model phase type FZP using Binary2 surfaces. As phase and amplitude type FZPs are analogous in focal distance measures, we implemented the FZP as a Binary2 surface to determine the light distribution pattern. Considering the dimensions we calculated for fabrication, we implemented the LED  $p$ -metal contact,  $p$ -GaN region,  $n$ -GaN region, sapphire substrate, and FZP using a mirror layer, a GaN cylinder with embedded source volume, a GaN rectangular volume, a sapphire rectangular volume, and a Binary2 surface, respectively. Positioning the LED active region at the FZP's first order focal distance would collimate the largest fraction of incident light, while subsidiary focal points would converge smaller fractions.

Having multiple focal points, the functionality of LED/FZP system can be tested by tracking the footprint of subsidiary focal points using regular optical microscopes, while measuring the beam angle of collimated output caused by main focal point requires more complex side-view microscopy. Hence, to simplify the required equipment for testing we aimed for detecting the image created by the  $f/3$  subsidiary focal point. Following the same strategy in the simulation, the  $f/3$  subsidiary focal point creates a high intensity spot at distance of 250  $\mu\text{m}$  from the surface [Fig. 3(a)] while the LED output without integrated FZP created a nonfocused result at the same distance [Fig. 3(b)].

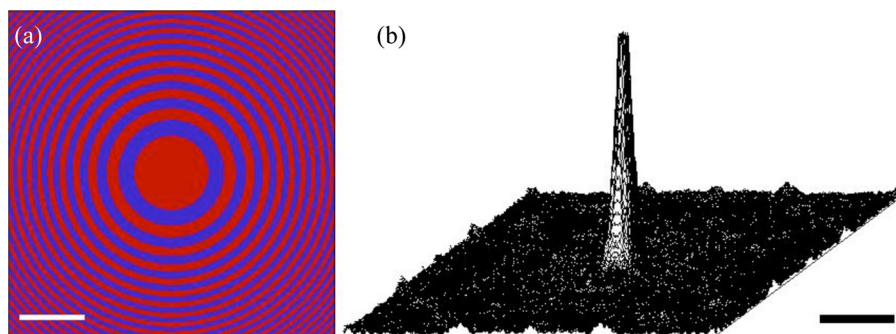


**Fig. 2** A Fresnel zone plate (FZP) implemented as obscurations in ZEMAX, The scale bar is 20  $\mu\text{m}$  (a), physical optic propagation (POP) analysis of FZP: 60- $\mu\text{m}$  waist Gaussian beam, illuminated through the designed FZP focuses at the desired 275  $\mu\text{m}$ ; the scale bar is 10  $\mu\text{m}$  (b)

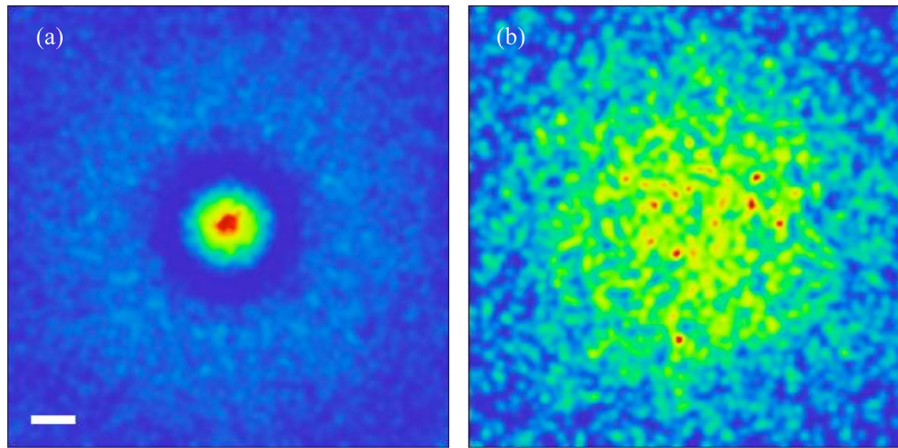


**Fig. 3** Simulated light intensity maps. LED structure modeled in nonsequential ZEMAX with integrated Binary2 surface as Fresnel zone plate (FZP), gives a focused spot caused by subsidiary  $f/3$  focal point at 250- $\mu\text{m}$  distance from the surface (a), while the LED without integrated Binary2 surface does not have the focusing behavior (b); the scale bar is 100  $\mu\text{m}$

## 2.4 Fabrication

### 2.4.1 Blue micro-LED fabrication

We started with epitaxial layers of InGaN/GaN grown on standard 2-in., 435- $\mu\text{m}$  thick *c*-plane sapphire wafers by metal organic vapor phase epitaxy (MOVPE) [Fig. 4(a)].<sup>3</sup> First, we defined the size and shape of each LED by evaporating a 120-nm thick layer of Ni to protect the *p*-GaN region (circular shape of 60- $\mu\text{m}$  diameter in this case) during the chlorine-based, inductively coupled plasma reactive ion etching (ICP RIE). We used AZ5214E (MicroChem Corp., MA), an image reversal photoresist, to gain sloped sidewalls and good lift-off results. The photoresist was spun coated, prebaked, exposed under a mask, hard baked, and finally flood exposed and developed resulting in a  $\sim 1.1\text{-}\mu\text{m}$  thick pattern. After development, the Ni layer was deposited by E-beam evaporation. The wafers were soaked in acetone for lift-off and then rinsed with iso propyl alcohol (IPA) and air dried [Fig. 4(b)]. To reach the *n*-GaN region and make metal connections, we used a chlorine-based ICP RIE to remove about 800 nm of top surface-*p*-GaN/multi quantum well stacks/and partially the *n*-GaN layer. After etching, the Ni layer was removed by soaking the wafer in a mixture of 1:3 HCl: HNO<sub>3</sub> [Fig. 4(c)]. To make metal connections for *p*-GaN, we used patterned AZ5214E photoresist, E-beam evaporated Ni:10 nm/Ag:70 nm/Au:150 nm layer, and performed a lift-off [Fig. 4(d)]. *p*-GaN contacts then were annealed at 500°C for 5 min. in nitrogen ambient. After a similar photolithography step, the *n*-GaN metal connections were deposited and lifted off as Ni/Al/Au:20/300/200 nm [Fig. 4(e)].

After the completion of LED metallization, the wafers were lapped and polished (Valley Design Corp., CA) in order to make the final LED chip thin enough to be embedded in a contact lens template, which resulted in an actual thickness of 273 to 276  $\mu\text{m}$  [Fig. 4(f)]. As the FZP must be fabricated on the lapped and polished side of the wafer, we needed to fabricate alignment marks for electron-beam lithography. We need to fabricate the marks from a material that can be imaged by scanning electron microscopy (SEM) easily and has good adhesion to sapphire. Chromium was a good option as was reported in a process to

mask sapphire during anisotropic etching and for making the alignment marks.<sup>13</sup> The alignment marks were designed large enough ( $\sim 10\ \mu\text{m}$ ) to allow photolithographic fabrication. Negative photoresist, nr7-1000 (MicroChem Corp., MA), was spun coated and patterned through a standard lithography process resulting in a 1.2- $\mu\text{m}$  thin film. A 100-nm thick layer of chromium was evaporated. Then the wafer was soaked in acetone for lift-off, rinsed with IPA and de-ionized (DI) water and air dried [Fig. 4(g)]. The wafer contained more than 2000 LED chips. To minimize losses during different tests, the wafer was saw-diced into smaller pieces by the following process. The sapphire wafer was mounted on a 4-in. silicon wafer as mechanical support by applying crystal bond. Using diamond resin blades (thermocarbon blades) mounted on a K&S dicing machine, we cut small, 9-mm squares. Conducting five pairs of perpendicular cuts, the wafer was soaked in acetone to release the pieces from the handle wafer. Pieces were then IPA/DI water rinsed, air dried and stored to be prepared for electron beam lithography (EBL).

### 2.4.2 FZP fabrication

A nominal FZP is comprised of concentric rings with progressively increasing radius and decreasing width moving away from the center. As the outermost ring in design was only  $\sim 650\ \text{nm}$ , we used electron beam lithography to create the structure with high fidelity. Starting with square pieces from the fabricated LED wafer, we baked the piece at 180°C for 3 min. to remove residual water from the surface. For better lift-off results we used a bilayer stack of E-beam resist with a more sensitive layer at the bottom that requires a lower exposure dose. Hence when exposed as a part of a bilayer stack, the bottom layer gives a wider line width for the same dose than the top layer, which results in an undercut profile that aids the lift-off. For the bottom layer, we spin coated the wafer piece with 7% P(MMA-MAA) copolymer (MicroChem Corp., MA) for a preferred thickness of 200 nm, and baked it at 180°C for 3 min., followed by spin coating of 2.5% 495PMMA A resist (MicroChem Corp., MA) in Anisole for a thickness of more than 100 nm as the top layer, followed by the same baking steps. As sapphire is not conductive, in order to prevent charging

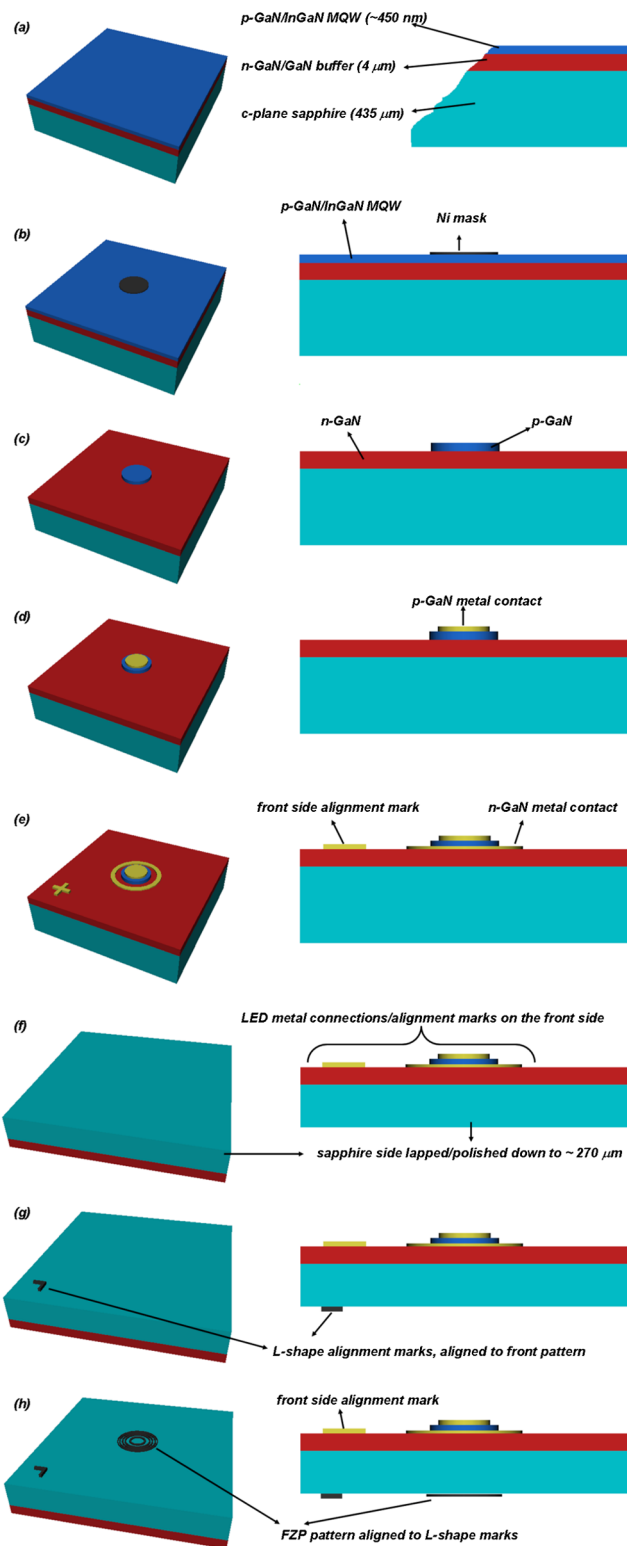


**Fig. 4** LED and Fresnel zone plates (FZP) fabrication process, starting with sapphire substrate with epitaxially grown layers of p-GaN/InGaN MQW/n-GaN/GaN buffer (a), Ni deposition as etch mask (b), Chlorine-based, inductively coupled plasma reactive ion etching (ICP RIE) of top layer (p-GaN/InGaN MQW) to reach the n-GaN region, then removing the Ni mask (c), p-contact metallization Ni/Ag/Au (d), n-contact and cross shape mark for backside alignment deposition (e), sapphire side lapped and polished down to  $\sim 270 \mu\text{m}$  (f), Aligned to front side cross marks, L-shaped alignment marks deposited using Cr (g), FZP opaque rings deposited after electron beam lithography (h).

up the surface during the E-beam lithography step, a very thin layer of Pd/Au (less than 10 nm) was sputtered using a small sputtering machine (Quorum, Q150RS). Then the piece was loaded on the electron beam lithography machine (JOEL JBX6300), and after proper alignment of FZP pattern in front of the LED mesa, it was exposed. After completing the electron beam writing, we etched the thin Pd/Au layer by dipping the sample in TFA Gold etchant (Transene Company, Inc.) for 10 s. The sample was developed in standard PMMA developer, 1:1 mixture of Methyl-Isobutyl-Ketone (J.T Baker Inc.) and IPA, then rinsed with IPA/DI water and air dried. Prior to depositing the metal layer the sample was attached to a 4-in. silicon wafer as a holder. To get minimal step coverage, we mounted the wafer on a custom made vertical wafer holder in the deposition chamber of an E-beam evaporator. 100 nm of chromium was deposited and the piece was then soaked in acetone for lift-off, leaving metal rings as opaque zones of FZP [Figs. 4(h) and 5].

Each wafer piece contained 100 LED chips that had to be separated for individual testing. Because of the fragility of sapphire and the crystal orientation used in our design, mechanical dicing/scribing would cause unacceptable chipping through the dicing path. To minimize the damage to the chips and fragile metal lines, we used a laser to scribe the pieces. The pieces were scribed down to  $\sim 200 \mu\text{m}$  using a DPSS laser at 266 nm (JPSSA, Inc., NH), and separated to single chips by applying manual pressure to the edges.

### 2.4.3 Template fabrication

As we will eventually assemble the LED chips on a flexible contact lens template, we used transparent polyethylene terephthalate (PET) to make templates for testing our chips. Starting with a 100- $\mu\text{m}$  thick, 100-sq. in. PET sheet (POLY-CROM, Inc.), 4-in. wafer shapes were cut using a CO<sub>2</sub> laser cutter. Wafers were cleaned in acetone/IPA/DI water and air dried. The fabrication had three lithography steps. First for patterning metal lines which provide electrical connection to LED after it is assembled. We used AZ4620 (MicroChem Corp.) for the first step. It was spin coated and patterned with thickness of  $\sim 4 \mu\text{m}$ , followed by evaporation of Cr:20 nm/Ni:80 nm/Au:200 nm. Wafers were then soaked in acetone to lift-off the metal layer and IPA/DI

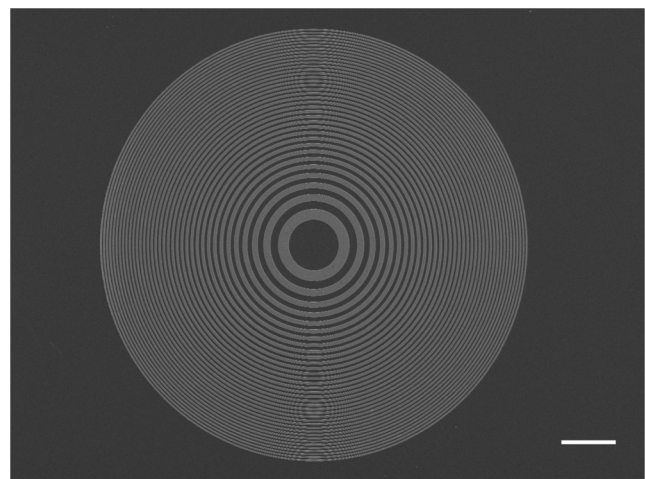


**Fig. 5** SEM image of a completed Fresnel zone plate; the scale bar is 25  $\mu\text{m}$ .

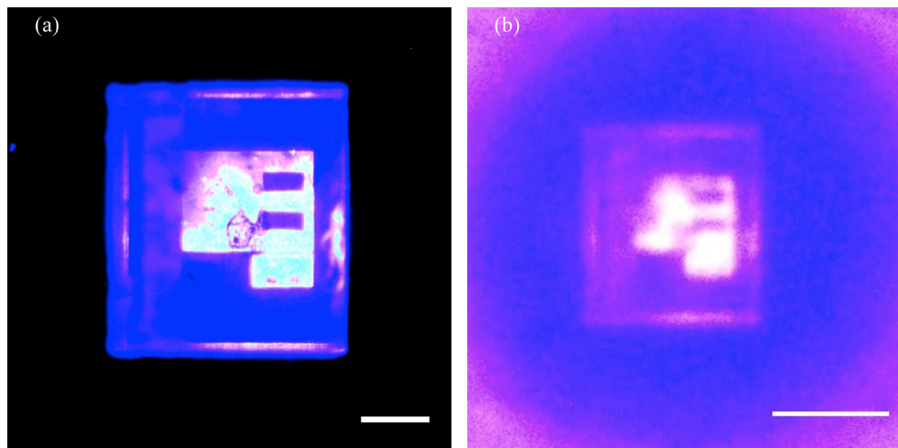


**Fig. 6** Optical microscope images of rectangular test LED chip with predetermined illumination pattern. The scale bar is 200  $\mu\text{m}$  (a), Fresnel zone plate (FZP) creates an upside down image of LED chip (which is  $\sim 5$  mm away of FZP) approximately at focal point. The FZP is visible as shadowed blue circle and LED chip image is recognizable as the rectangle with bright illuminated pattern (we flipped the image to make the object and image comparison more convenient). The scale bar is 50  $\mu\text{m}$  (b).

water rinsed and air dried. The second lithography step was to passivate some of the metal interconnects that could potentially be shorted by LED metal pads after assembly. A  $\sim 2\text{-}\mu\text{m}$  layer of SU8-2 was spin coated and patterned to make this insulation. Finally, for making a housing for the LED chip, we spin coated and patterned a  $\sim 25\text{-}\mu\text{m}$  layer of SU8-25 with  $900 \times 900 \mu\text{m}^2$  openings for LED chips.

#### 2.4.4 LED assembly

The LED assembly was done using an aided self-assembly process. Lead free,  $60^\circ\text{C}$  eutectic solder (Indalloy 19, Indium Corp.) was melted in a 100-mL beaker while immersed in ethylene glycol (EG). Templates were rinsed with acetone/IPA and air dried. Metal pads on the template were coated with solder using pipette flow. To minimize the surface oxidation of solder bumps and maintain clean surfaces, templates were immediately immersed in a glass Petri dish containing 25 mL of EG and 10  $\mu\text{L}$  of HCL. The LED chips were then placed on corresponding spots on the template manually using a tweezer. Afterwards the Petri dish was heated in order to melt the solder. As the

solder melted, the LED chip self-aligned and connected to the template's metal pads. After the solder was cooled down, the template with assembled LED was rinsed with IPA and air dried to be ready for further testing.

### 3 Results

In addition to integrating zone plates in front of LED structures, we also fabricated zone plates on bare sapphire substrates to optimize the fabrication parameters for E-beam lithography. As our first test we put a sapphire wafer with FZP patterns 5 mm away from an illuminating LED chip with a complex pattern [Fig. 6(a)] under an optical microscope (ML7000, MEIJI TECHNO Co., Japan). Initially we focused on the FZP surface, and then by moving the microscope objective, we changed the objective focal plane and were able to detect an upside down image of LED chip in front of the FZP [Fig. 6(b)].

As the simulation results of LED with integrated FZP indicate, we expect the zone plate to focus the light at a point in front of the structure while the LED without zone plate should have a diverging output. To test the functionality of the FZP, we compared the output of LEDs with FZP

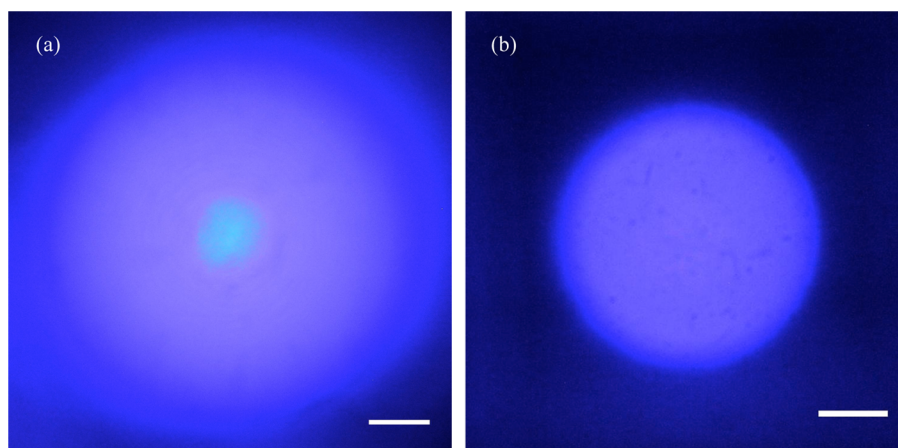


**Fig. 7** LED with integrated Fresnel zone plate (FZP) output, focused at 230  $\mu\text{m}$  from FZP surface, caused by  $f/3$  subsidiary focal point (a), LED without integrated FZP output at 230  $\mu\text{m}$  from LED surface (b); scale bars are 50  $\mu\text{m}$ .

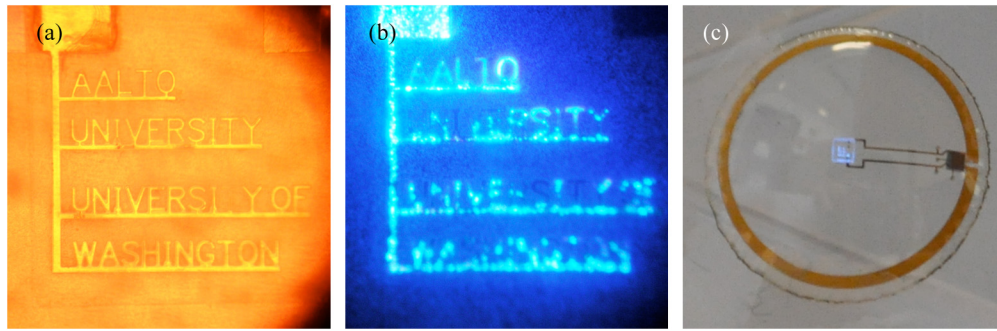


**Fig. 8** Optical microscope image of predetermined text, “AALTO UNIVERSITY, UNIVERSITY OF WASHINGTON”, fabricated on LED by shaping the electrode pattern (a), optical microscope image of the LED emitting the predetermined pattern upon application of a bias current (b), the LED chip assembled on contact lens with radio and antenna, and turned on wirelessly (c)

integrated in front and LEDs without integrated FZP. The assembled LEDs were put under the microscope objective, while current was fed by probe station probe tips. The LED with integrated FZP produces a bright spot resulting from  $f/3$  subsidiary focal point at  $\sim 230 \mu\text{m}$  from FZP surface [Fig. 7(a)], which is close to what the simulations predicted ( $250 \mu\text{m}$ ). The LED without Zone plate has a

diverging uniform output cross section [Fig. 7(b)]. These experiments verified the FZP function successfully.

We also assembled an LED with predetermined text [Fig. 8(a)–8(b)] on a contact lens platform through the process reported in Ref. 3. In addition to the LED chip, the contact lens contained integrated antenna and radio chip for power harvesting and control. As shown in Fig. 8(c), we were able to wirelessly power and control this LED on a contact lens.



**Fig. 9** Two-level phase type Fresnel zone plate (FZP) with 40% efficiency (left), Four-level phase type FZP with 81% efficiency (right), which needs two additional electron beam lithography (EBL)/etching mask deposition/anisotropic etching steps. Adopted from Ref. 15

#### 4 Discussion

We were able to verify the functionality of the designed zone plates and detect the LED output focused by the  $f/3$  subsidiary focal point at the expected location; however, there are several parameters that could be optimized in future implementations to make the LED/FZP system output more efficient. To maximize the amount of LED light output collected from the sapphire surface, two solutions may be considered. The first is to increase the FZP diameter (up to  $200 \mu\text{m}$  in our case). This will decrease the smallest ring width down to  $300 \text{ nm}$ , which can easily be achieved by accessible electron beam lithography equipment. This would limit the number of pixels on the contact lens unless a single FZP is used for multiple pixels. The second way is to thin the substrate down to  $\sim 150 \mu\text{m}$ , which is commercially available, and design the lens with new focal distance, defined by new thickness, but the same diameter.

There is a 10% limit for diffractive efficiency of the amplitude-type zone plate, which could be increased to 40% by using a phase-type FZP. This is achievable by adding a sapphire etch step of  $308 \text{ nm}$  to make a  $\pi$  phase shift. This etch could be performed after deposition of chromium layers (exactly as in the amplitude-type design) and utilizing them as sapphire etch masks.  $\varphi$  would be the phase shift occurring using wavelength of  $\lambda$  after passing a layer of material with thickness of  $t$  and refractive index of  $n$ .<sup>12,14</sup>

$$\varphi = 2\pi(n - 1)t/\lambda. \quad (2)$$

The efficiency could still be enhanced by increasing the  $\pi$  phase shift quantization. For example, increasing the phase change quantization from a two level ( $0$  and  $\pi$ ) to four levels ( $0, \pi/3, 2\pi/3, \pi$ ) (Fig. 9), would increase the efficiency up to 81%, reducing the subsidiary focusing effect.<sup>15,16</sup> This approach adds two more electron beam lithography/etch mask deposition/anisotropic sapphire etching steps to the

process, compared to a two level phase type FZP. It also requires precise alignment. Note that special care is needed to protect the phase pattern during the molding process in the contact lens for example by bonding a flat transparent thin glass layer to the Fresnel zone after etching.

Decreasing the LED size—for example 22- $\mu\text{m}$  pitch has already been demonstrated<sup>17</sup> increases the pixel count on the display chip, decreases electrical power consumption per pixel, and optically makes the LED more similar to a point source that gives more uniformity in the collimated output.

## 5 Conclusions

We have demonstrated the successful design, fabrication, and testing of micro-LEDs with integrated FZPs. Such LEDs may be used in a contact lens display platform to form in-focus images on the retina from components placed directly on the surface of the cornea. We have also demonstrated the integration of LEDs emitting predetermined text patterns on a contact lens and the wireless operation of the system. In order to simplify the fabrication process, we used amplitude-type diffractive patterns; however, in order to achieve higher efficiencies, phase-type patterns must be implemented in the system. The FZPs may be placed in front of a single pixel or a group of pixels for imaging.

FZPs are perhaps some of the simplest diffractive patterns that can be integrated in a contact lens but they demonstrate the promise of contact lenses for integration of sophisticated diffractive optical elements for correcting and augmenting vision surpassing what might be feasible with conventional refractive optical elements.

## Acknowledgments

We would like to thank M. Ali, M. Sapanen, S. Suihkonen, and Harri Lipsanen of Aalto University for providing epitaxially grown wafers, and for their help with process development for LED fabrication and patterning; A. Lingley for providing help with template fabrication and the chip assembly process; R. Bojko for extensive help with E-beam lithography; and the staff of University of Washington Microfabrication Facility for their help in process development.

## References

1. M. Billingham and T. Starner, "Wearable devices: new ways to manage information," *Computer* **32**(1), 57–64 (1999).
2. J. Pandey et al., "A fully integrated RF-powered contact lens with a single element display," *IEEE Trans. Biomed. Circuits Syst.* **4**(6), 454–461 (2010).
3. A. Lingley et al., "A single-pixel wireless contact lens display," *J. Micromech. Microeng.* **21**(12), 125014 (2011).
4. F. L. Pedrotti, L. S. Pedrotti, and L. M. Pedrotti, *Introduction to Optics*, 3rd ed., p. 426, Pearson Prentice Hall, upper saddle river, NJ(2007).
5. Jeon et al., "Polymer microlens arrays applicable to AlInGaN ultraviolet micro-light-emitting diodes," *IEEE Photon. Technol. Lett.* **17**(9), 1887–1889 (2005).

6. Zhu et al., "Microlens array on flip-chip LED patterned with an ultraviolet micro-pixelated emitter," *IEEE Photon. Technol. Lett.* **23**(15), 1067–1069 (2011).
7. Khizar et al., "Nitride deep-ultraviolet light-emitting diodes with microlens array," *Appl. Phys. Lett.* **86**(17), 173504 (2005).
8. Choi et al., "Nitride micro-display with integrated micro-lenses," *Solid State Phys.* **2**(7), 2903–2906 (2005).
9. Choi et al., "GaN micro-light-emitting diode arrays with monolithically integrated sapphire microlenses," *Appl. Phys. Lett.* **84**(13), 2253–2255 (2004).
10. A. Holmberg, "Nanofabrication of zone plate optics for compact soft x-ray microscopy," Doctoral Thesis, (Royal Institute of Technology 2006).
11. Menon et al., "Experimental characterization of focusing by high-numerical-aperture zone plates," *J. Opt. Soc. Am. A* **23**(3), 567–571 (2006).
12. A. Michette, "Zone and phase plates, Bragg-Fresnel optics," in *Handbook of Optics*, McGraw-Hill, New York, **3** (2000)
13. J. Kang et al., "Inductively coupled plasma reactive ion etching of sapphire using C2F6- and NF3-based gas mixtures," *Mater. Sci. Semicond. Process.* **11**(1), 16–19 (2008).
14. M. E. Motamedi et al., "Micro-optics integration with focal plane arrays," *Opt. Eng.* **36**(5), 1374–1382 (1997).
15. K. Yamada et al., "Multilevel phase-type diffractive lenses in silica glass induced by filamentation of femtosecond laser pulses," *Opt. Lett.* **29**(16), 1846–1848 (2004).
16. H. O. Sankur et al., "Micro-optics development in the past decade," *Proc. SPIE* **4179**, 30–59 (2000).
17. H. W. Choi et al., "High-resolution 128  $\times$  96 nitride microdisplay," *IEEE Electron. Dev. Lett.* **25**(5), 277–279 (2004).



**Ramin Mirjalili** received his BSc and MSc degrees from Sharif University of Technology, Tehran. He studied electrical and petroleum engineering in his undergraduate studies. He continued his studies in electronics with a focus on microelectronics circuitry design and biosensors. He joined Professor Parviz's group as a PhD student in September 2009. He started with working on template and components fabrication of bionic contact lens heterostructure and with main emphasis on microdisplays. He has been working on devising a method for producing in-focus images from them.



**Babak A. Parviz** received his graduate degrees from the University of Michigan in Ann Arbor. From 2000 to 2001 he was with Nanovation Technologies Inc. as a device designer and a product manager working on integrated photonics. He joined the Department of Chemistry and Chemical Biology at Harvard University as a postdoctoral research fellow in 2001. At Harvard, he was involved in research on developing novel nanofabrication technologies, self-assembled systems, low-cost biosensing, and using organics for electronics and MEMS. He joined the UW Electrical Engineering Department as a faculty member in October 2003. He is currently the associate director of the Micro-scale Life Sciences Center at the University of Washington. He is a founding member of the American Academy of Nanomedicine; a senior member of the IEEE; and a member of the American Association for Advancement of Science, American Chemical Society, Association for Research in Vision and Ophthalmology, and Sigma Xi.